

SOOT FORMATION IN HYDROCARBON DIFFUSION FLAMES

J. Houston Miller, Anthony Hamins, and Trudy A. Kohout

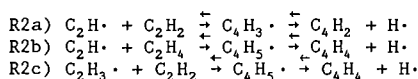
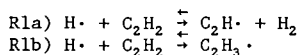
Department of Chemistry
The George Washington University
Washington, DC 20052

Kermit C. Smyth^a and W. Gary Mallard^b

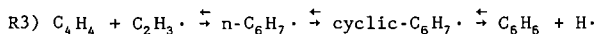
^aCenter for Fire Research and ^bCenter for Chemical Physics
The National Bureau of Standards
Gaithersburg, MD 20899

INTRODUCTION:

The chemistry of the combustion of simple hydrocarbons to form carbon dioxide and water has been extensively studied and is generally well established [1]. Our level of understanding of the chemistry which leads to the formation of polynuclear aromatic hydrocarbons (PAH) and soot particles is less fully developed. Numerous modelling efforts have been applied to the analysis of concentration data collected in shock tubes and premixed flames [2-6]. Although there are many proposed routes involving specific hydrocarbon free radicals, these models do share some common features. Fuel molecules are converted to relatively high concentrations of acetylene. Two-carbon atom free radicals formed during this pyrolysis process, or by hydrogen atom reactions with acetylene, can react with acetylene to form four carbon atom species.



Four-carbon atom species can react with either acetylene or two-carbon atom radicals to form six-carbon atom radicals, which may cyclize into aromatic structures. Finally, the cyclic radicals can lose or add hydrogen to form stable aromatic hydrocarbons such as benzene. For example:



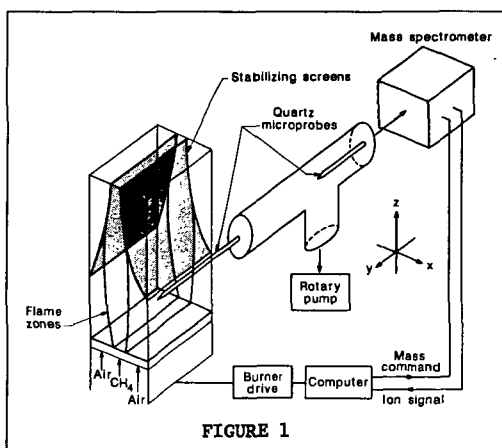
Analogous growth processes lead to the formation of larger ring structures and finally soot particles. The aromatic structures are believed to act as "islands of stability" along the reaction pathway [6], in effect providing a measure of irreversibility to the process. Because the thermodynamic stability of the aromatic structures increases with size, these subsequent ring formation steps occur more rapidly than the earlier ones. Our emphasis, therefore, has been on the chemical formation route for the first aromatic ring with the goal of verifying specific mechanisms for this process. A model

must not only account for observed concentrations of intermediate hydrocarbons but also for their net rate of production as a function of flame position.

In our laboratory, specific attention has been given to identifying the important chemistry leading to the formation of the key precursor molecules to soot particle formation in diffusion flames. To achieve this goal measurements of the important intermediate gas phase species, temperature, and velocity fields have been required. The results of these studies provide a comprehensive data base with which to examine the phenomenon of soot particle inception in flames. In this paper, a review of some of the results of these studies will be given along with a discussion of areas of future interest.

Experimental Approach

A study of the structure of laminar diffusion flames has been undertaken in which spatially detailed measurements of the gas phase species, velocity, and temperature fields have been obtained. The majority of the work has been carried out for flames burning methane in air, although some preliminary work has been done for ethylene/air diffusion flames. Only the methane flame results will be described in this paper. The design of the burner has been described elsewhere in detail and will only briefly be summarized here [7]. The fuel flowed through a central slot located between two air slots. The resulting flame sheets are symmetric about the plane through the center of the burner (see Figure 1). The burner assembly was mounted on a two-dimensional computer-controlled, micrometer stage so that movement laterally, through the flame sheets, and vertically was possible. Lateral profiles of temperature, velocity, and species concentrations were collected at relatively high spatial resolution (0.2 mm) at a series of heights (consecutive profiles were taken every 2 mm).



Species concentrations were determined by a direct sampling quartz microprobe system with mass spectrometric analysis. A probe following the

design of Fristrom and Westenberg [8] was inserted into the flame parallel to the fuel/air flow separators. Mass spectrometer signals were calibrated against room temperature mixtures, and the resulting calibration factors were corrected for the temperature dependence of the molecular flow through the sampling probe orifice. In a related series of experiments, molecular iodine from a side arm on the probe was mixed with the flame gas sample just inside the orifice [9]. Iodine reacts quantitatively with methyl radicals to form methyl iodide, which could survive the remainder of the sampling train and be detected mass spectrometrically.

Results

Figure 2 illustrates the temperature and velocity fields for the methane/air flame supported on the Wolfhard/Parker slot burner. Shown in solid lines are isothermal contours determined from thermocouple profiles⁷. Also shown are streamlines of convective velocity calculated from the two measured velocity components. The streamlines exhibit trajectories which begin in the lean region of the flame, cross the high temperature reaction zones, and continue into the fuel-rich regions.

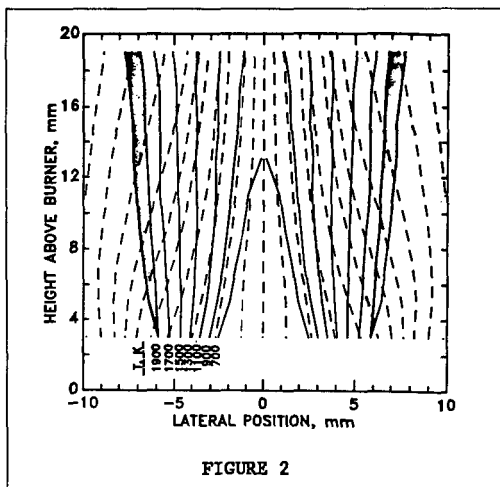


Figure 3 shows mass-spectrometric profiles of the concentrations of a variety of stable flame species at a height of 9 mm above the burner. A number of points are noteworthy in comparing Figures 2 and 3. First, the concentrations of oxygen and methane approach zero near the high temperature reaction zone at ± 6 mm from the burner centerline, where the concentration of water is a maximum. Second, the high concentration of nitrogen near the burner centerline reveals that significant entrainment of air (as shown by the velocity measurements in Fig. 1) and diffusion of nitrogen toward the burner centerline occur.

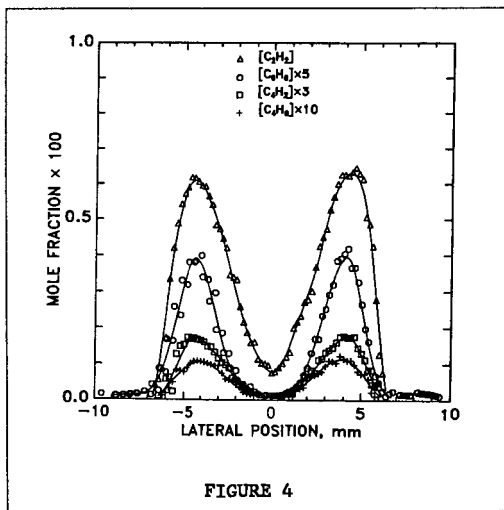
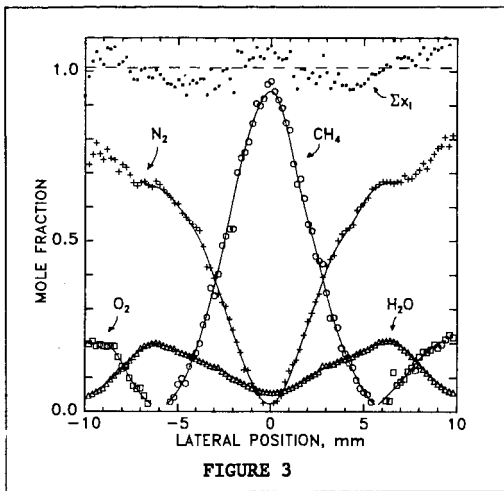


Figure 4 illustrates profiles collected at 9 mm above the burner surface for several intermediate hydrocarbons: acetylene, benzene, diacetylene, and butadiene. Peak concentrations at this height for these species are 6200, 800, 570, and 110 parts per million, respectively. Profiles for a large

number of additional intermediate hydrocarbons were obtained, and all have concentration maxima in the same region of the flame.

In addition to the probe studies described above, we have also applied optical diagnostic techniques to the study of the methane/air flame. Figure 5 compares the relative OH concentration profiles at various heights above the burner surface with profiles of C_2 fluorescence. Also shown is the Rayleigh light scattering signal for three flame heights. The absence of distinct peaks in the scattering signal profiles indicates that large soot particles are not detectable below 15 mm in the methane/air flame. The C_2 fluorescence is attributed to laser photolysis of large hydrocarbon molecules. Figure 5 shows that the OH concentration maximum occurs further away from the burner centerline (in more lean regions of the flame) than the area where hydrocarbons such as benzene and soot particles are observed.

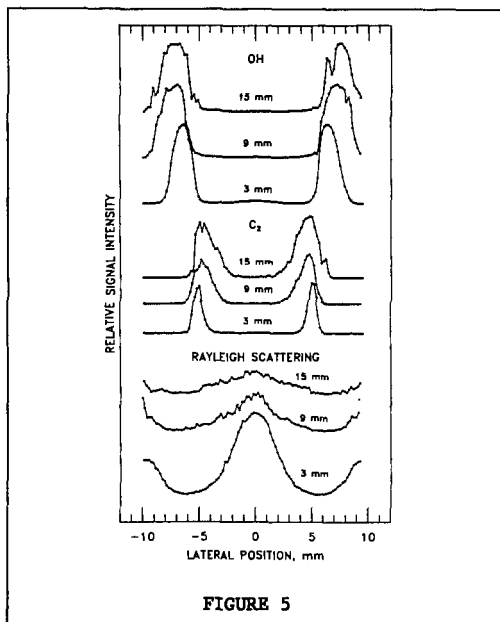


FIGURE 5

Data Analysis and Discussion

A laminar flame is a steady-state system: the value of any macroscopic variable (such as a species concentration) does not change with time at a particular spatial location [10]. Because there is a flow of material into and out of a given volume element due to mass transport, there must be a corresponding change in species' concentrations due to chemical reactions:

$$R_i = \nabla[N_i (v + V_i)]. \quad (1)$$

Here, R_i is the net chemical rate, N_i is the species concentration, v is the mass average (convective) velocity, and V_i is the diffusion velocity of the species into the local mixture. All of the quantities on the right-hand side of Eq. 1 have been experimentally determined (N_i and v) or can be calculated directly from the experimental data (V_i).

Figure 6 illustrates the calculation of the chemical production rate, R_i , for acetylene at heights of 5 and 13 mm above the burner surface. Low in the flame, the rate profile exhibits a maximum destruction value near the high temperature, primary reaction zone, and a formation feature slightly toward the fuel side. This peak in the production rate is located on the lean, higher temperature side of the observed concentration peak (see Figure 4). Higher in the flame, the production rate is diminished by a new destruction feature (see arrow). This new destruction feature spatially overlaps an observed profile maximum for small soot particles, and this feature is believed to be due to acetylene participation in soot surface growth processes [10].

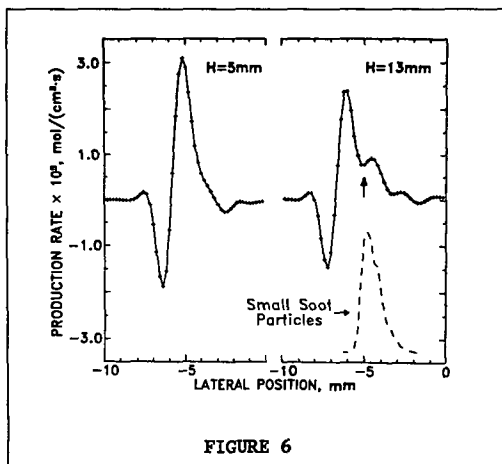
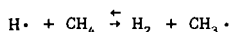


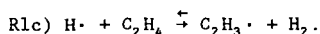
FIGURE 6

The concentration and production rate data have been used to critically evaluate proposed mechanisms for hydrocarbon condensation chemistry in the methane flame. For example, our data allows us to select between competitive reactions during specific growth steps in the formation of benzene. In the Introduction, alternative processes involving two, four, and six carbon-atom free radicals were suggested for the sequence leading from acetylene to benzene. For a given reaction to be important, its maximum forward rate must be faster than the observed production rate of the product benzene. For example, both ethynyl radicals and vinyl radicals can be formed by hydrogen atom reaction with acetylene. For these calculations, the concentration of

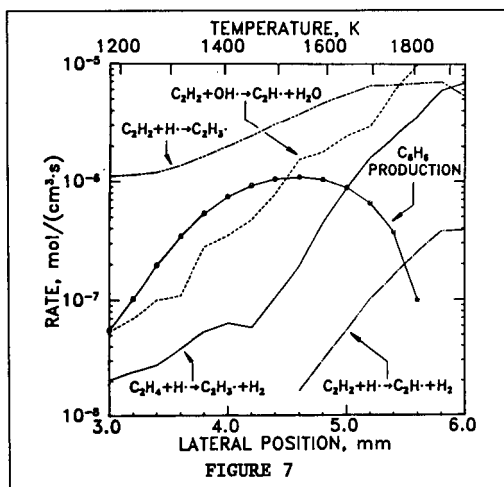
hydrogen atoms was determined by assuming equilibrium with methane in the reaction [10]:



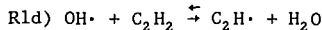
In Figure 7, the formation rates of these radicals via reactions 1a and 1b are compared with the observed net benzene formation rate. As this figure indicates, the ethynyl radical, $\text{C}_2\text{H} \cdot$, is produced too slowly to account for the observed rate of the formation of benzene in the methane flame. In contrast, the vinyl radical, $\text{C}_2\text{H}_3 \cdot$, formed through hydrogen atom addition to acetylene, is formed fast enough to account for our benzene rate data. Another route to vinyl formation is hydrogen abstraction from ethylene:



We have recently developed a method for distinguishing the individual contributions to the mass 28 signal from CO , N_2 , and C_2H_4 . Thus, the importance of reaction 1c) in the formation of benzene can be determined. The forward rate of R1c is plotted in Figure 7. Near the flame reaction zone, the magnitude of vinyl formation through R1c exceeds the observed net forward formation rate of benzene. Thus, in the methane flame, vinyl formation through both acetylene and ethylene can contribute to aromatic ring formation.



In a previous paper on the production rate calculations¹⁰, we concluded that the vinyl radical was the key two-carbon radical in the formation sequence leading to benzene. This result was predicated on the assumption that oxygen containing radicals such as OH were not involved directly in this process. However, OH abstraction of hydrogen from acetylene to form ethynyl is a fast reaction [11] and should be considered in our analysis. We have therefore added reaction 1d)



to the two-carbon radical formation processes plotted in Figure 7. Because laser induced fluorescence provides a determination of only the relative hydroxyl radical concentration, it is necessary to scale the profile results to a reasonable estimate of the actual OH concentration. To this end, the peak OH concentration was taken to be that predicted by the NASA combustion equilibrium code for methane/air mixtures at the local equivalence ratio, ≈ 0.7 , and the temperature, 2030 K, where the fluorescence maximum is observed [12]. This estimate should prove to be conservative: Mitchell et al. have found super-equilibrium concentrations for OH in fuel-rich regions of methane/air diffusion flames [13]. As Figure 7 demonstrates, formation of ethynyl from OH reactions with acetylene is fast enough to account for the observed benzene formation rate.

Further tests of benzene formation mechanisms will focus on competitive routes to four-carbon molecule formation (R2a-R2c). A critical concern will be the relative concentrations of vinyl and ethynyl radicals. If the vinyl radical concentrations far exceed the ethynyl radical concentrations, as has been observed in pre-mixed acetylene flame results [14], then processes such as reaction 2c will be far more important than the ethynyl radical reactions such as 2a or 2b. Reliable estimation or measurement schemes for these radicals remains as one of the great challenges in unravelling diffusion flame chemistry.

References

1. I. Glassman and P. Yaccarino, Eighteenth Symposium (International) on Combustion, The Combustion Institute, 1175 (1981).
2. J. Warnatz, Eighteenth Symposium (International) on Combustion, The Combustion Institute, 69, (1981).
3. T. Tanzawa and W.C. Gardiner, Jr., J. Phys. Chem. **84**, 236 (1980).
4. M.B. Colket, III, Chemical and Physical Processes in Combustion, Eastern States Section of the Combustion Institute, Paper 53, November 1985.
5. J.A. Cole, J.D. Bittner, J.P. Longwell, and J.B. Howard, Combustion and Flame **56**, 51 (1984).
6. M. Frenklach, J.W. Clary, W.C. Gardiner, and S.E. Stein, Twentieth Symposium (International) on Combustion, The Combustion Institute, 887 (1984).
7. K.C. Smyth, J.H. Miller, R.C. Dorfman, W.G. Mallard, and R.J. Santoro, Combustion and Flame **62**, 157 (1985).
8. R.M. Fristrom and A.F. Westenberg, Flame Structure, McGraw-Hill, New York, 1965.
9. J.H. Miller and P.H. Taylor, Combustion Science and Technology, in press.
10. J.H. Miller, W.G. Mallard, and K.C. Smyth, Twenty-first Symposium (International) on Combustion, The Combustion Institute, in press.
11. W. Tsang and R.F. Hampson, Journal of Physical and Chemical Reference Data **15**, 1087 (1986).
12. S. Gordon and B.J. McBride, NASA SP-273, 1971.
13. R. Mitchell, A.F. Sarofim, L.A. Clomburg, Combustion and Flame **37**, 201 (1980).
14. P.R. Westmoreland, D. Sc. Dissertation, Massachusetts Institute of Technology, 1986.